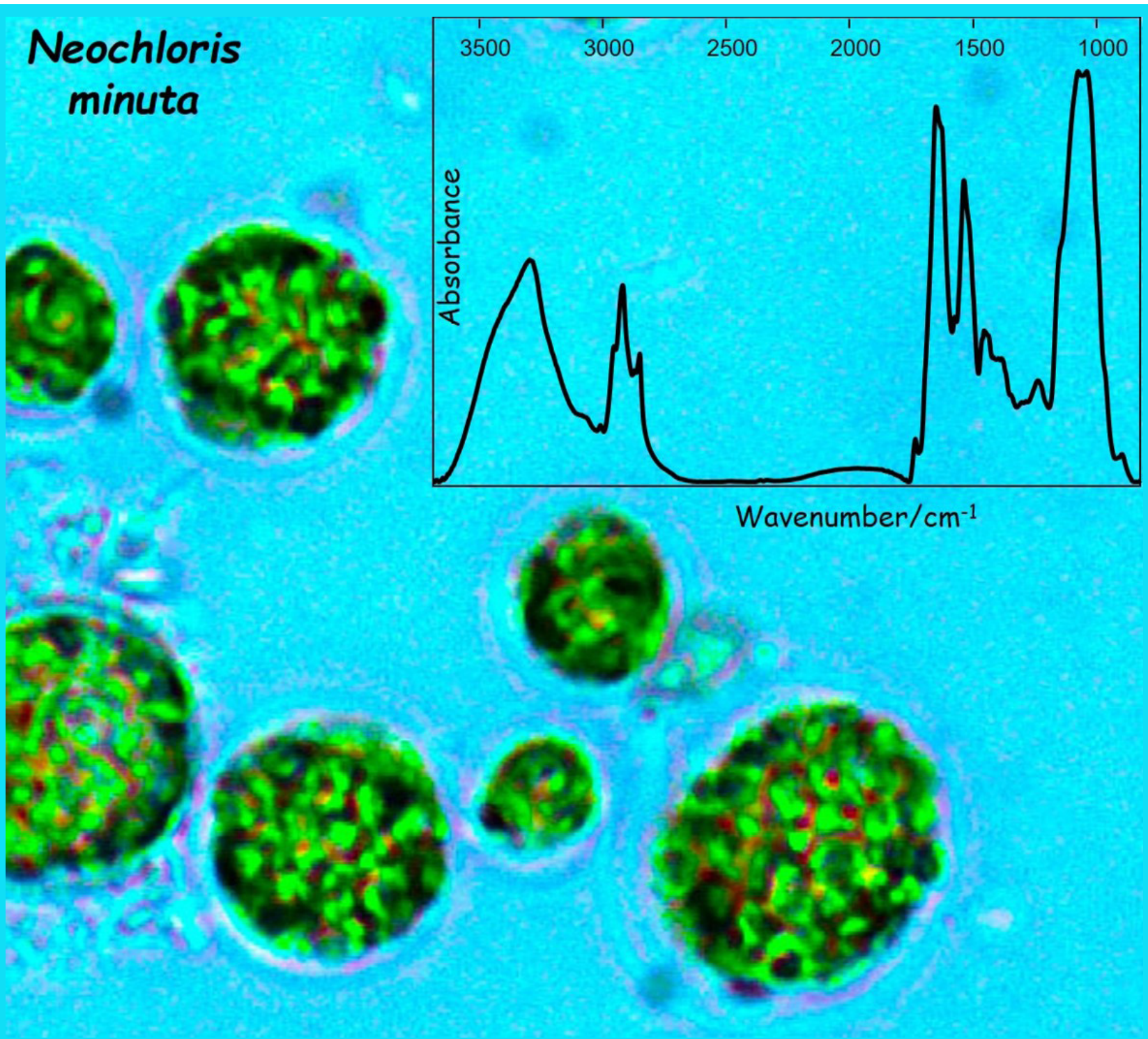
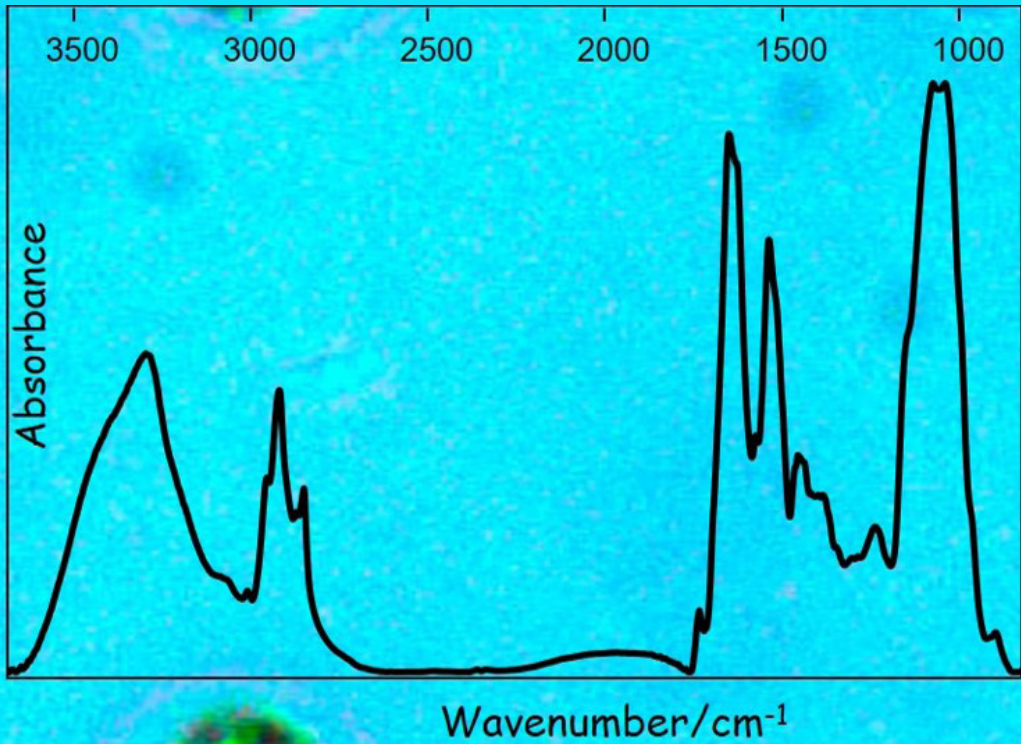


Frontiers

in Science, Technology, Engineering and Mathematics

*Neochloris
minuta*



Research Paper

Starch, Lipid, and Protein Accumulation in Nutrient-Stressed Microalgal Cells Studied Using Fourier Transform Infrared Microscopy.

Gary Hastings^{1,*}, Jodian Thomas¹, Keillor Witt¹, Dimitrios Giarikos², and Reza Razeghifard²

¹Department of Physics and Astronomy, Georgia State University, Atlanta, Georgia 30303, USA;

²Department of Chemistry and Physics, Nova Southeastern University, Fort Lauderdale, Florida 33314, USA. *Corresponding author, Gary Hastings, Email: g Hastings@gsu.edu

Received April 11, 2018, revised May 23, 2018, accepted May 23, 2018

Publication Date (Web): May 24, 2018

© Frontiers in Science, Technology, Engineering and Mathematics

Abstract

Microalgae are fast growing organisms that can be used as feedstock for the production of biofuels. The metabolism of microalgae can be manipulated by exposing them to different environmental conditions for favoring the accumulation of lipids, carbohydrates or proteins. For example, a change in growth conditions can cause the accumulation of large amounts of lipids, representing an opportunity for biodiesel production. Monitoring changes in the composition of microalgal cells is therefore important in assessing new growth conditions. However, at present, most techniques are time consuming, invasive and expensive. Here we have used FTIR microscopy to quantify lipid, protein, and starch accumulation in *Neochloris minuta* cells grown in the presence and absence of nitrogen. Under nitrogen deprivation the cellular lipid composition increases by a factor of 2.4, the cellular protein concentration decreases by ~60% while the starch concentration is unaltered. These estimates of biochemical composition were derived using a variety of analytical methods, and form the basis for establishing to what extent FTIR microscopy can be used as a probe of cellular biochemical composition. We find that the distribution of materials in *Neochloris minuta* cells estimated directly from the FTIR spectra compare favorably with that estimated using these other analytical methods. FTIR spectroscopy is shown to be a versatile and easy-to-use tool for estimating distributions of biological materials in microalgal cells.

Keywords

Microalgae, FTIR microscopy, infrared spectroscopy, *Neochloris minuta*, algal lipids, algal starch, algal protein.

Introduction

Microalgae are fast growing photosynthetic organisms that can be manipulated to overproduce important products/chemicals that can be used, for example, in biofuel production (Tiwari et al 2013). Cultivation mode and growth conditions are shown to affect the yield and biochemical composition of biomass (Morales et al 2018; Li et al 2008). The monitoring of the biochemical composition of biomass, for example lipid accumulation in oleaginous microorganisms is crucial to develop and validate new growth conditions, but at present the majority of the available techniques are time consuming, invasive and expensive. Here we have used FTIR microscopy to rapidly quantify lipid, protein, and starch accumulation in *Neochloris minuta* (*N. minuta*) (Arce et al 2008; Deason et al 1991) cells grown in the presence and absence of nitrogen (+N and -N, respectively).

Removing nitrogen from the growth medium often causes a substantial increase in the lipid content of algal cells that correlates with a decrease in the cellular protein and/or starch content (Li et al 2008; Dean et al 2010; Stehfest et al 2005). FTIR spectroscopy has often been used to probe changes in cellular composition induced by nitrogen starvation (Dean et al 2010; Stehfest et al 2005; Pistorius et al 2009).

We have chosen to work with *N. minuta* cells, in part because they have not been widely studied in the past, and in part because of their favorable growth characteristics in our photo-bioreactor.

The lipid starch and protein content of cells used in this study have been estimated using a variety of analytical techniques (see Materials and Methods section). The results on cellular composition derived from these studies can be directly compared to estimates based on the FTIR spectra obtained for the cells. In this way the applicability of the methods used to analyze the FTIR spectra of the cells can be established. With the establishment of these FTIR spectral analysis methods this approach could find utility in the compositional analysis of a wide range of both eukaryotic and prokaryotic cell types.

In this manuscript FTIR spectra were obtained for *N. minuta* cells grown in the presence and absence of nitrogen. These spectra were used to quantify lipid, protein, and starch accumulation in the intact cells. It is shown that the ratios of these

materials in the intact cells estimated directly from the FTIR spectra compare favorably with their percent values obtained from the chemical analysis of dried cells using other analytical methods.

Materials and Methods

N. minuta (UTEX#776) cells were obtained from the culture collection of the University of Texas. The cells were cultured in a modified Bristol medium with the amounts of nutrients increased by six times and supplemented with trace metal ions of BG-11 medium (Anderson et al 2005). Cells were grown in glass bottles with continuous sterile air bubbling for agitation. Cells were illuminated from both sides with T5 high output fluorescent lighting systems (EnviroGro) each having 4 light tubes. The incident light intensity on the surface of the bottle was $180 \pm 20 \mu\text{E m}^{-2} \text{ s}^{-1}$ measured by a MQ-200 Quantum Sensor (Apogee Instruments Inc. Logan, UT). The light sources were switched on and off by a time-controlled outlet strip to give cultures 14 hours of daylight. The *N. minuta* cells were first collected from agar plates and grown for 5 days in +N medium at $30 \pm 2 \text{ }^\circ\text{C}$. The algal cells were collected by removing the growth medium by centrifugation at 5000 rpm for 5 min at 15°C using a Beckman Coulter Optima Max-XP refrigerated centrifuge. The cell pellets were washed with milli-Q water before they were regrown for an additional 5 days in +N or -N media. Overnight sedimentation and centrifugation were then applied to harvest and store the concentrated cells at $4 \text{ }^\circ\text{C}$.

For FTIR measurements samples were thawed and 1 mL of each sample was centrifuged at 10,000 rpm for 5 minutes using a table top centrifuge. The supernatant was discarded while the pellet was resuspended in double distilled water. This “rinsing” was repeated three times. The pellet after the final rinse was resuspended in a minimal volume of double distilled water in order to achieve a cell density that was appropriate for transfection FTIR microscopy experiments. Several 2- μL drops of the resuspended samples were placed on low emissivity (IR reflective) windows (Kevley Scientific) and allowed to dry under weak vacuum for 10 minutes at room temperature.

FTIR microscopy measurements were undertaken in transfection mode using a Varian 7000 FTIR spectrometer coupled to a Varian UMA600 IR microscope, as described previously (Hastings et al 2008). The microscope utilizes on-axis, matched 15X

Schwarzschild objectives and condenser. IR light is detected using a single element 0.25x0.25 mm mercury cadmium telluride (MCT) detector. Spectral resolution was set at 4 cm^{-1} . The IR light impinging on the sample was limited by variable apertures (typically set to 0.1x0.1 mm). Spectra were collected at many points on the dried sample spots. Spectra collected were only considered for analysis if the amide I absorption band was less than ~ 1.0 in optical density units.

FTIR microscopy is not strictly necessary for the measurements undertaken here, and good data could be obtained using macroscopic methods (not shown). The microscopic approach does allow very small sample volumes to be considered, however, which we anticipate will be valuable in our future analysis of dilute samples at very early stages of growth.

Total triacylglyceride (TAG) concentrations were measured using the infinity triglycerides reagent (TR-22421 Fisher Scientific). Initially 10 mg of dried algae was suspended in 1 mL of 4 M NaOH and heated at 80°C for 1 h. The solution was then neutralized with 2 M HCl. 180 μL of sample was mixed with 1.5 mL of triglycerides reagent in a 2 mL microcentrifuge tube and incubated on a shaker at 37 °C for 10 min and 200 rpm. Absorbance readings were taken at 600 nm and the total concentration of TAGs was calculated from a calibration graph constructed from different concentrations of glyceroltripalmitate (T5888 Sigma-Aldrich). The 10 mg/mL glyceroltripalmitate standard was treated with the same saponification procedure explained above prior to the reaction with the infinity triglycerides reagent.

Starch was measured by digesting 0.3 mL of algal sample prepared for TAG measurements with 50 μL of amyloglucosidase enzyme (A7095 Sigma-Aldrich) in 1 mL (total volume) of 50 mM acetate buffer (pH=4.8) on a shaker at 60 °C for 30 min and 200 rpm. The amyloglucosidase enzyme was dialyzed three times against 50 mM acetate buffer (pH=4.8) at 4 °C overnight. 0.1 mL of the digested sample was mixed with 0.9 mL of glucose reagent and incubated at 37°C for 5 min. The starch concentration was calculated by converting the absorbance reading at 340 nm to glucose concentration using $\epsilon_{\text{NADH}} = 6.22 \text{ mM}^{-1} \text{ cm}^{-1}$. As a control, a calibration graph can be constructed from a 10 mg/mL solution of starch made in 1 mL of 4 M NaOH and heated at 80 °C for 5 min. The starch solution needs to be neutralized with 2 M HCl prior to the digestion with the amyloglucosidase enzyme.

The nitrogen contents for the algal samples were determined by triplicate elemental analyses of the dried

algae by Micro-Analysis Inc., Wilmington, DE. The % protein in the algal cells was calculated using 4.78 as the nitrogen-to-protein conversion factor defined for microalgae.¹¹

Results and Discussion

The lipid protein and starch percentages obtained from the chemical analysis of the biomass extracted from dried *N. minuta* cells grown in the presence (+N) or absence (-N) of nitrogen for 10 days are outlined in Table 1. *N. minuta* cells have a high starch content (41-45%) independent of whether the cells are grown under +N or -N conditions (Table 1). The protein contribution to the total biomass decreases by a factor of 2.54 for -N grown cells, while the lipid content increases by a factor of 2.36 (Table 1). The lipid to protein ratio is 0.386 under +N conditions, and 2.32 under -N conditions. That is, the lipid to protein ratio increases by a factor of ~ 6 for cells grown under -N conditions compared to that under +N conditions. The starch to protein ratio is 1.58 under +N conditions, and 3.66 under -N conditions. So the starch to protein ratio increases by a factor of 2.32 under -N conditions compared to that under +N conditions. The lipid to starch ratio is 0.244 under +N conditions, and 0.634 under -N conditions. So the lipid to starch ratio increases by a factor of 2.6 under -N conditions, compared to that under +N conditions.

The data in Table 1 is useful in the analysis and interpretation of bands in FTIR spectra obtained for these cells grown under two different conditions.

Figure 1A shows FTIR spectra, and calculated second derivative spectra obtained for *N. minuta* cells grown under +N and -N conditions. The spectra in figure 1A covers the whole mid-IR region, (3800-800 cm^{-1}). Expanded views of the spectra in figure 1A are shown in figure 1B-D.

Figure 1C shows an expanded view of the amide I and II absorption bands that are well known to be due to protein absorption (Surewicz et al 1996). Since the spectra in figure 1 are scaled to the area under these “protein” bands the spectra will therefore provide information on the other components of the cellular biomass on a “per-unit-protein” basis. It should be noted that other studies have normalized spectra differently. For example, some groups simply normalize spectra to the intensity of the peak of the amide I band (Driver et al 2015), while others have

used the area under the amide II absorption band to normalize spectra (Pistorius et al 2009).

Amide I and II Absorption Bands

In figure 1C the amide I band is broad, displaying two prominent peaks at 1657 and 1627 cm^{-1} as indicated by the negative peaks in the second derivative spectra. Weaker bands are also suggested at 1697 and 1685 cm^{-1} . The bands underlying the broad amide I band are generally associated with different elements of protein secondary structure. In particular, the 1657 and 1627 cm^{-1} bands are well known to be associated with α -helix and β -sheet secondary structures, respectively. The weak feature at 1685 cm^{-1} may be associated with sheets or turns (Surewicz et al 1996; Susi et al 2015). It is possible to assess the secondary structural content of a protein by fitting the amide I band to a series of underlying bands that can be associated with different secondary structural elements. However, such a procedure is of little value here, as whole cells contain a large number of different proteins, each with their own secondary structural elements contributing to the spectra. The amide II absorption band displays two peaks at 1545 and 1518 cm^{-1} that probably correspond to the 1657 and 1627 cm^{-1} amide I features. The amide II bands are known to relate to protein secondary structure details, but in a less clear cut fashion than the amide I contributions.¹² Notice that peaks in the second derivative spectra in figure 1C are observed at the same frequencies for cells grown under +N and -N conditions. This indicates that the protein secondary structure contributions are the same or similar in the cells grown under the different conditions, even although the contribution of protein to the overall cellular biomass is decreased under -N growth conditions.

In figure 1 the spectra are normalized so that the area under the amide I and II absorption bands are similar, so the spectra are approximately normalized to the total protein content of the cell. Bear in mind, however, that the protein contribution to the total cellular biomass is 2.54 times lower for the cells grown under -N conditions (Table 1).

Second derivative spectra are shown in figure 1 in order to indicate peak positions and to help resolve multiple peaks underlying broad absorption bands. The intensity of the negative peaks in the second

derivative spectra do not relate linearly to the concentration of molecular species in the cell.

Finally, note that the shape of the amide I and II absorption bands will differ in FTIR experiments undertaken in transmission mode, as found previously in FTIR studies of eukaryotic cells (Hastings et al 2008).

Lipid Absorption Bands

For -N grown *N. minuta* cells the protein content drops by a factor of 2.54. Since the spectra in figure 1 are normalized to protein content, then the FTIR bands associated with non-protein biomolecules will be magnified by 2.54. This is indicated in Table 1, where the change in the lipid to protein and starch to protein ratios are presented. The data in Table 1 suggest that much of the changes in the FTIR spectra for cells grown under +N and -N conditions will come from changes in lipid and starch contributions to the cellular biomass, with changes due to alterations in lipid composition dominating.

Lipids give rise to intense FTIR bands in the 3020-2850 cm^{-1} spectral region, and figure 1B shows a magnified view of spectra collected for +N and -N grown *N. minuta* cells in this region. In this spectral region bands are associated mainly with C-H stretching vibrations associated with the lipid hydrocarbon chain (Derenne et al 2013). Proteins also contribute in this region but to a lesser extent (Hastings et al 2008). This latter point is clear based on a consideration of the spectrum for cells grown in the presence of nitrogen, but scaled to the main lipid absorption bands at 2925 and 2853 cm^{-1} (spectrum in semi-transparent red in figure 1B). This latter spectrum has a greater protein to lipid ratio but is still quite similar in shape to the spectrum for cells grown under -N conditions. The additional intensity in the peaks near 2960 and 2873 cm^{-1} could be due to C-H stretching of protein methyl groups.

For FTIR spectra of cells it has been estimated that the protein contribution to the area under the bands in the ~2990-2850 cm^{-1} region is equal to about 40% of the area under the amide II band (Pistorius et al 2009). Based on the data in figure 1A, it is apparent that the protein contribution to the area under the bands in the 2990-2850 cm^{-1} region, for cells grown under -N conditions, is small.

Table 1. Biomass composition after 10 days of growth of *N. minuta* cells.

Algae	Lipid %	Starch %	Protein %	Lipid/Protein	Starch/Protein	Lipid/Starch
<i>N. minuta</i> , +N	11±0.8	45±5.6	28.5±0.2	0.386	1.58	0.244
<i>N. minuta</i> , -N	26±1.1	41±2.8	11.2±0.1	2.32	3.66	0.634
Ratio (-N/+N)	2.36	0.91	0.39	6.01	2.32	2.60

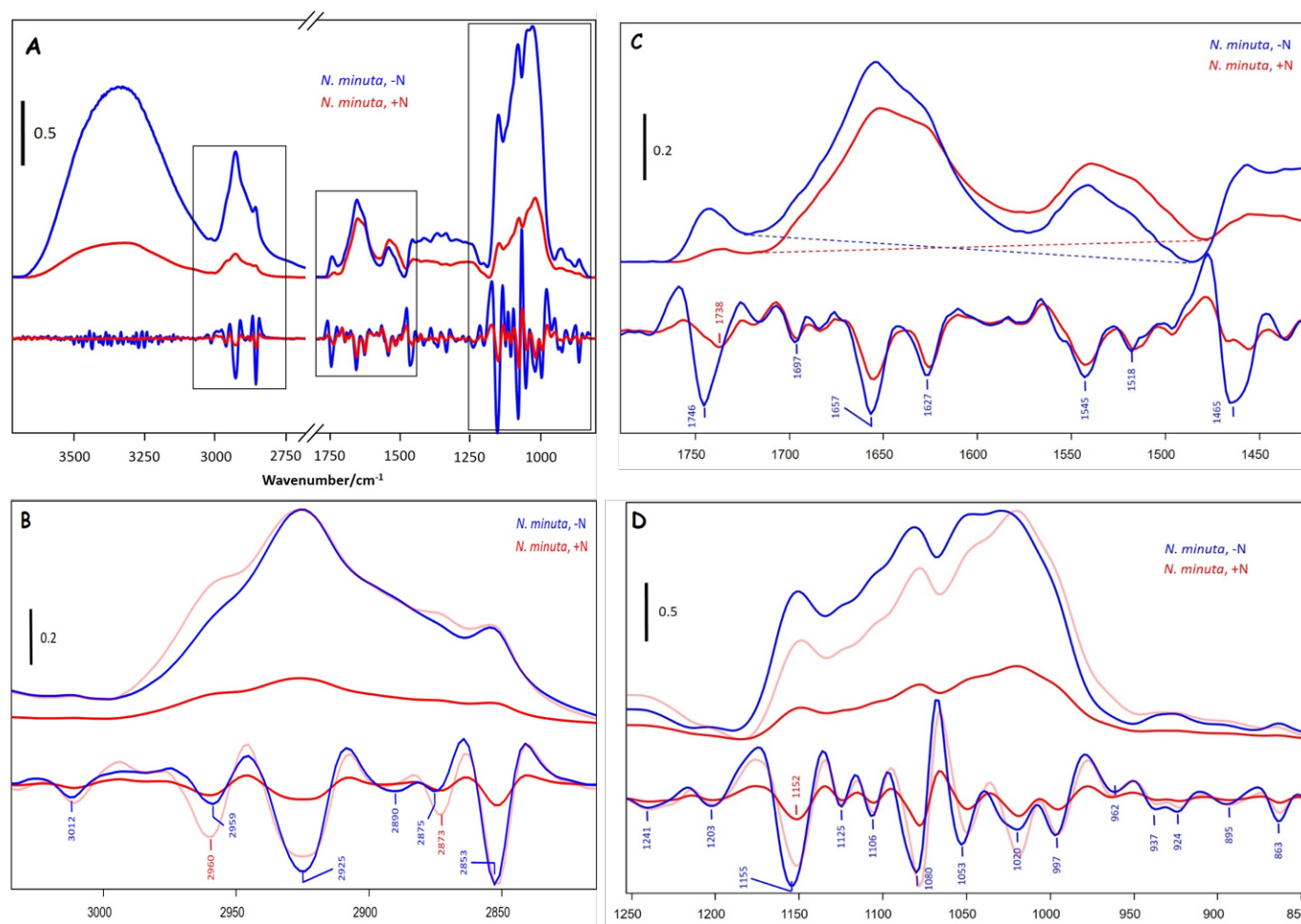


Figure 1. Infrared spectra obtained for *N. minuta* cells grown in media containing (red) and depleted (blue) of nitrogen. In (A) spectra covering the 3800-800 cm^{-1} region are shown. The spectra in (A) were baseline corrected using the rubber band algorithm as implemented in OPUS 7.0 software from Bruker Optics. This procedure did not significantly alter the relative band areas discussed in this manuscript. Second derivative spectra are also shown (scaled by a factor of 100). Expanded views of the spectra in (A) are shown in B-D. Absorption spectra are scaled so that the area under the amide I and II absorption bands are similar. The area considered is specified by the dotted lines in (C). In (B), (D) scaled versions of spectra obtained for +N grown cells are also shown (semitransparent red).

In figure 1B, the intense bands at 2925 and 2853 cm^{-1} are associated with antisymmetric and symmetric methylene vibrations [$\nu_{\text{as}}(\text{CH}_2)$ and $\nu_{\text{s}}(\text{CH}_2)$] of the

lipid hydrocarbon chains. The band near 2959 cm^{-1} is associated with $\nu_{\text{as}}(\text{CH}_3)$ modes, with a weaker band associated with the $\nu_{\text{s}}(\text{CH}_3)$ mode at 2875 cm^{-1}

(Derenne et al 2013). The ratio of the area under the bands associated with methylene and methyl vibrations has been proposed to relate to the length of the lipid hydrocarbon chain for the spectra of pure lipids. Implementation of this methodology is likely not of value here as the spectra hint at multiple types of different lipids contributing to the spectra (see below). The band near 3012 cm^{-1} is associated with unsaturated acyl chains ($\nu_{\text{as}}(\text{HC}=\text{CH})$ vibrations), and its intensity can be used to assess the degree of saturation of the lipid hydrocarbon chain (Derenne et al 2013).

For cells grown under $-N/+N$ conditions the area under the whole band profile in the $3000\text{--}2830\text{ cm}^{-1}$ region is $51.8/12.4$, respectively. So the area ratio is 4.2 (figure 2A). Taking into account that protein absorption contributes equally to the spectra obtained under both growth conditions (area ~ 4.0) then the calculated change in the area ratio, corrected for protein contributions, is ~ 6 . Thus the change in the lipid to protein ratio, as assessed from the area under the bands in $3000\text{--}2830\text{ cm}^{-1}$ region, for cells grown under $-N/+N$ conditions, is ~ 6 . This estimate is in excellent agreement with the data listed in Table 1 derived using independent analytical methods. Comparing the absorption of the 2925 and 2853 cm^{-1} bands for cells grown under both $+N$ and $-N$ conditions leads to a calculated ratio of 4.6 and 4.4 (figure 2A), respectively, so the peak absorption ratios by themselves cannot be used to give a reliable estimate of the change in the lipid to protein ratio for cells grown under the two different growth conditions.

The band at 3012 cm^{-1} is due to lipid acetyl C–H absorption, and provides a measure of the degree of saturation of the lipid hydrocarbon chain. The ratio of the area under the 3012 cm^{-1} bands for the different growth condition is ~ 4.0 . This increase in unsaturated lipids in $-N$ grown cells has not been verified using other analytical techniques so far.

Noticeably, the bands in the spectra in figure 1B are very broad, considerably broader than the bands in the same spectral region found in FTIR spectra of pure lipids (Derenne et al 2013), indicating a broad range of lipid types, with different degrees of saturation. The broad range of lipids contributing to the bands in figure 1B, makes a more quantitative analysis difficult at present.

Ester Lipids

In figure 1C an intense band is observed near 1746 cm^{-1} for cells grown under $-N$ conditions. For cells grown under $+N$ conditions a considerably weaker band is observed at 1738 cm^{-1} . Bands in the $1750\text{--}1730\text{ cm}^{-1}$ region are associated with lipid ester carbonyl ($\text{C}=\text{O}$) vibrations (Derenne et al 2013). The area under the 1738 cm^{-1} band for $+N$ grown cells is a factor of six less than the area under the 1746 cm^{-1} band for the $-N$ grown cells (figure 2B). This is precisely as expected from the data in Table 1, which indicates a factor of six change in the lipid to protein ratio when cells are grown in the absence of nitrogen. The difference in the peak position of the lipid ester band under the different growth conditions might indicate some difference in the lipid composition of $-N$ grown cells. This idea will be tested in future GCMS studies of fatty acids obtained by derivatization of lipids extracted from *N. minuta* cells.

Starch Absorption Bands

In *N. minuta* cells grown under $-N$ conditions, the starch to protein ratio is 3.66 , compared to 1.58 for cells grown under $+N$ conditions. Thus a 2.32 increase in the ratio for cells grown under $-N$ conditions (Table 1). Therefore, for the FTIR spectra of *N. minuta* cells grown under the different conditions, normalized to protein content, one expects large differences in the spectra in regions where starch absorption bands appear. In figure 1 the spectra obtained for cells under $+/-N$ conditions are scaled to protein content and very large differences in the spectra are observed, particularly in the $1200\text{--}950\text{ cm}^{-1}$ region, which is shown expanded in figure 1D. Lipids, including phospholipids, also absorb in the $1200\text{--}1000\text{ cm}^{-1}$ region, so one should be careful in assigning absorption bands to specific biomolecules. Starch is also known to display an absorption band near 2930 cm^{-1} (Sacithraa et al 2013), which could also complicate the analysis outlined above related to estimation of the lipid to protein ratio based on the bands in the $3000\text{--}2800\text{ cm}^{-1}$ region.

In the $\sim 1200\text{--}950\text{ cm}^{-1}$ region for cells grown under both conditions, bands are observed at 1020 , 1080 and 1155 cm^{-1} , and shoulders at 997 and 1053 cm^{-1} . These features are well known absorption features found in spectra associated with various starches (Sacithraa et al 2013; Warren et al 2016), although lipids also give rise to absorptions at similar frequencies.

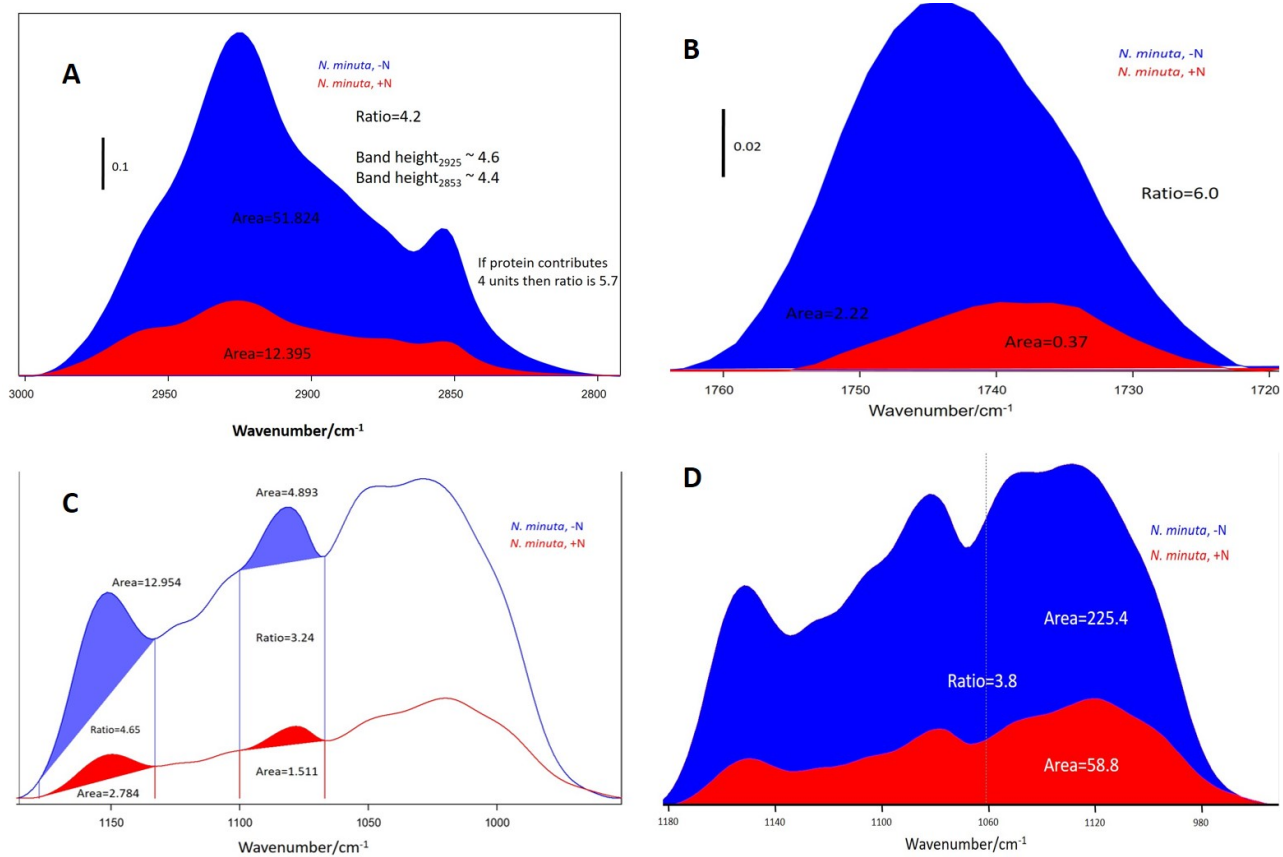


Figure 2. Infrared spectra obtained for *N. minuta* cells grown in media supplemented (red) and depleted (blue) of nitrogen, in the (A) 3000–2780, (B) 1770–1715 and the (C), (D) 1200–900 cm^{-1} region. The spectra were baseline corrected to consider only the region of interest. The band areas used to calculate the various ratios are indicated. Areas were calculated using the integrate function in OPUS 7.0 software from Bruker Optics

For *N. minuta* cells normalized to protein content, one expects a ~ 2.3 increase in the intensity of spectral bands associated with starch. The change in the starch to protein ratio can be estimated based on the area under, for example, the 1155 or 1080 cm^{-1} bands. The ratio of the area under the two bands for cells grown under $-N$ and $+N$ conditions is 4.7 and 3.2, respectively (figure 2C). This is considerably larger than the factor of ~ 2.3 listed in Table 1. In addition, by considering the total area under the broad spectral feature covering the 1180–900 cm^{-1} region, one finds that the ratio in the area for cells grown under $-N/+N$ is still 3.8 (figure 2D). Thus a consideration of the area underlying the absorption bands in the 1200–1000 cm^{-1} region seems to overestimate the starch to protein ratio, as assessed using other analytical techniques. Of course, given that lipids also contribute to absorption changes in the 1200–1000 cm^{-1} region, and that the

lipid/protein ratio increases by a factor of ~ 6 upon nitrogen removal, a calculated area ratio of ~ 3.8 might be reasonable.

In figure 1A a broad, featureless absorption increase is observed between 1460–1240 cm^{-1} , and is typical of that found in the infrared spectra of some starches (tapioca starch in reference by Lourenco et al 2004). This feature is easily visualized in figure 1A. The absorption associated with this feature in figure 1A is 0.23/0.1 for cells grown under $-N/+N$ conditions, respectively. This ratio in absorption of ~ 2.3 is exactly that estimated from other analytical techniques (Table 1), it would therefore appear that this broad absorption feature is an excellent direct measure of the starch levels in the cells grown under $+N/-N$ conditions. To our knowledge this broad feature is a new “starch marker” that has not been suggested in the literature previously.

Given the broad and featureless nature of this absorption it is obviously associated with a large number of underlying vibrational modes. Even in the infrared spectra of simply glucose, already a large number of bands are observed in the 1460–1240 cm^{-1} range (Heise et al 2002) that are associated with primarily deformational modes involving hydrogen, such as O-H and C-H bending vibrations (Dauchez et al 1994).

Conclusions

Here we demonstrate that FTIR micro-spectroscopy is a fast, reliable and non-invasive method to monitor and analyze lipid, carbohydrate, and protein accumulation in intact algal cells.

Acknowledgements

KW acknowledges support from an undergraduate summer research fellowship from the molecular basis of disease (MBD) program at Georgia State University. RR acknowledges support from PFRDG index 335400 awarded by Nova Southeastern University.

References

- Anderson, R. A. *Algal Culturing Techniques*. Elsevier, 2005.
- Arce, G. & Bold, H (1958) Some Chlorophyceae from Cuban Soils. *American Journal of Botany* **45**, 492-503
- Dauchez, M. et al (1994) Force-field and vibrational spectra of oligosaccharides with different glycosidic linkages—Part I. Trehalose dihydrate, sophorose monohydrate and laminaribiose. *Spectrochimica Acta Part A: Molecular Spectroscopy* **50**, 87-104
- Deason, T. R., Silva, P. C., Watanabe, S. & Floyd, G. L (1991) Taxonomic status of the species of the green algal genus *Neochloris*. *Plant Systematics and Evolution* **177**, 213-219
- Dean, A. P., Sigee, D. C., Estrada, B. & Pittman, J. K. (2010) Using FTIR spectroscopy for rapid determination of lipid accumulation in response to nitrogen limitation in freshwater microalgae. *Bioresource technology* **101**, 4499-4507
- Derenne, A., Claessens, T., Conus, C. & Goormaghtigh, E. Infrared Spectroscopy of Membrane Lipids. In: *Encyclopedia of Biophysics* (ed Gordon C. K. Roberts) , pp. 1074-1081, 2013
- Driver, T. et al. (2015) Metabolic responses of eukaryotic microalgae to environmental stress limit the ability of FT-IR spectroscopy for species identification. *Algal Research* **11**, 148-155
- Hastings, G., Wang, R., Krug, P., Katz, D. & Hilliard, J. (2008) Infrared microscopy for the study of biological cell monolayers. I. Spectral effects of acetone and formalin fixation. *Biopolymers* **89**, 921-930
- Heise, H. M. Glucose Measurements by Vibrational Spectroscopy. In: *Handbook of Vibrational Spectroscopy* Vol. 5, (eds J M Chalmers & P R Griffiths), pp. 3280-3294, 2002
- Li, Y. Q., Horsman, M., Wang, B., Wu, N. & Lan, C. Q. (2008) Effects of nitrogen sources on cell growth and lipid accumulation of green alga *Neochloris oleoabundans*. *Applied microbiology and biotechnology* **81**, 629-636
- Lourenco, S. O., Barbarino, E., Lavin, P. L., Marque, U. M. L. & Aidar, E. (2004) Distribution of intracellular nitrogen in marine microalgae: Calculation of new nitrogen-to-protein conversion factors. *Eur J Phycol* **39**, 17-32
- Morales, M., Sánchez, L. & Revah, S. (2018) The impact of environmental factors on carbon dioxide fixation by microalgae. *FEMS Microbiol Lett* **365**, fnx262-fnx262
- Pistorius, A. M. A., DeGrip, W. J. & Egorova-Zachernyuk, T. A. (2009) Monitoring of Biomass Composition From Microbiological Sources by Means of FT-IR Spectroscopy. *Biotechnology and Bioengineering* **103**, 123-129
- Sacithraa, R., Madhanmohan, M. & Vijayachitra, S. Quantitative Analysis of Tapioca Starch using FT-IR Spectroscopy and Partial Least Squares. International Conference on Innovations In: *Intelligent Instrumentation, Optimization and Electrical Sciences ICIIIOES*, pp. 29-33, 2013
- Stehfest, K., Toepel, J. & Wilhelm, C. (2005) The application of micro-FTIR spectroscopy to analyze nutrient stress-related changes in biomass composition of phytoplankton algae. *Plant Physiol Bioch* **43**, 717-726
- Surewicz, W. & Mantsch, H. Infrared Absorption Methods for Examining Protein Structure. In: *Spectroscopic methods for determining protein*

- structure in solution* (ed HA Havel), pp. 135-162, 1996
- Susi, H. & Byler, D. M. (1986) Resolution-enhanced Fourier transform infrared spectroscopy of enzymes. *Methods Enzymol* 130
- Tiwari, A. & Pandey, A. Algal Biofuels. In: *Natural and Artificial Photosynthesis: Solar Power as an Energy Source* (ed Reza Razeghifard) Ch. 9, pp. 243-266, 2013
- Warren, F. J., Gidley, M. J. & Flanagan, B. M. (2016) Infrared spectroscopy as a tool to characterise starch ordered structure—a joint FTIR–ATR, NMR, XRD and DSC study. *Carbohydrate Polymers* **139**, 35-42

Citation:

Gary Hastings, Jodian Thomas, Keillor Witt, Dimitrios Giarikos and Reza Razeghifard (2018) Starch, lipid, and protein accumulation in nutrient-stressed microalgal cells studied using Fourier transform infrared microscopy, *Frontiers in Science, Technology, Engineering and Mathematics*, **Volume 2**, Issue 3, 121-129.
